

Supporting information

Unlocking a Modular Gd-DOTBA Platform via Tetramaleimide Click Chemistry for High-Performance MRI

Xinhui Xiao,^{a,c†} Shiyao Wang,^{a†} Peijie Guan,^{a,c} Zhiqiang Wang^{a*} and Lixiong Dai^{b,c*}

^aDepartment of Radiology, Wenzhou Hospital of Integrated Traditional Chinese and Western Medicine, Wenzhou, Zhejiang 325000, China

^bDepartment of Radiology, The Second Affiliated Hospital and Yuying Children's Hospital of Wenzhou Medical University, Wenzhou, Zhejiang 325027, China

^cWenzhou Key Laboratory of Biophysics, Wenzhou Institute, University of Chinese Academy of Sciences, Wenzhou, Zhejiang 325000, China

†These authors contributed equally to this work.

*E-mail: dailx@wiucas.ac.cn; cn_boy2000@wmu.edu.cn

Table of Contents

Reagents and Equipment	S1
HPLC Methods	S1
Synthesis	S2
Determination of Relaxivity.....	S3
Determination of Gd Metal Content of Gd-DOTBA-Mal-Cys	S3
Kinetic Stability Assessment	S4
Cell Cytotoxicity	S4
Acute and Subacute Toxicity Assessment.....	S5
Animal Model	S5
<i>In vivo</i> MRI Studies.....	S5
Biodistribution	S6
Table S1 Relaxivity of Gd-DOTBA-Mal-Cys ^a	S7
Fig. S1 ¹ H NMR spectrum of DOTBA in D ₂ O.	S7
Fig. S2 ¹³ C NMR spectrum of DOTBA in D ₂ O.	S8
Fig. S3 ¹ H NMR spectrum of Eu-DOTBA in D ₂ O.	S8
Fig. S4 Analytical HPLC spectrum of Gd-DOTBA-Mal.....	S9
Fig. S5 ESI-MS of Gd-DOTBA-Mal.	9
Fig. S6 Analytical HPLC spectrum of Gd-DOTBA-Mal-Cys.	S10
Fig. S7 High resolution ESI-MS of Gd-DOTBA-Mal-Cys.	S10
Fig. S8 Cell viability of LX-2, 293T, and HeLa cells after 24h incubation with varying concentrations of Gd-DOTBA-Mal-Cys.	S11
Fig. S9 Representative H&E-stained sections of liver and kidney from Balb/c mice treated with PBS, Gd-DOTA, or Gd-DOTBA-Mal-Cys (0.1 mmol/kg) in acute (1 day) and subacute (30 days) toxicity studies. Scale bar = 100 μm.	S11
Fig. S10 <i>T</i> ₁ -weighted MR images of normal mice at different time points after intravenous injection of Gd-DOTBA-Mal-Cys at 3.0 T magnetic field.....	S12
Fig. S11 Biodistribution of the Gd-DOTBA-Mal-Cys.....	S12

Fig. S12 HE-staining of the kidney after UUO 2days and UUO 9 days (scale = 200 μm)	S13
References	S14

Reagents and Equipment

All chemicals and reagents were used as received from commercial sources unless otherwise noted. 4-Dimethylaminopyridine 4-methylbenzenesulfonate (DMTMM), 1-(2-Aminoethyl)-1H-pyrrole-2,5-dione, L-cysteine and zinc chloride (ZnCl_2) were purchased from Energy Chemical. Gd-DOTA (Gadoteric acid, HENGRUI) were obtained from clinics. Phosphate buffer saline (PBS, 1 \times , pH 7.4), Matrigel, Dulbecco's Modified Eagle Medium (DMEM), RPMI-1640 medium, fetal bovine serum (FBS) and trypsin-EDTA were purchased from Gibco. Cell Counting Kit-8 (CCK-8) was sourced from Beyotime.

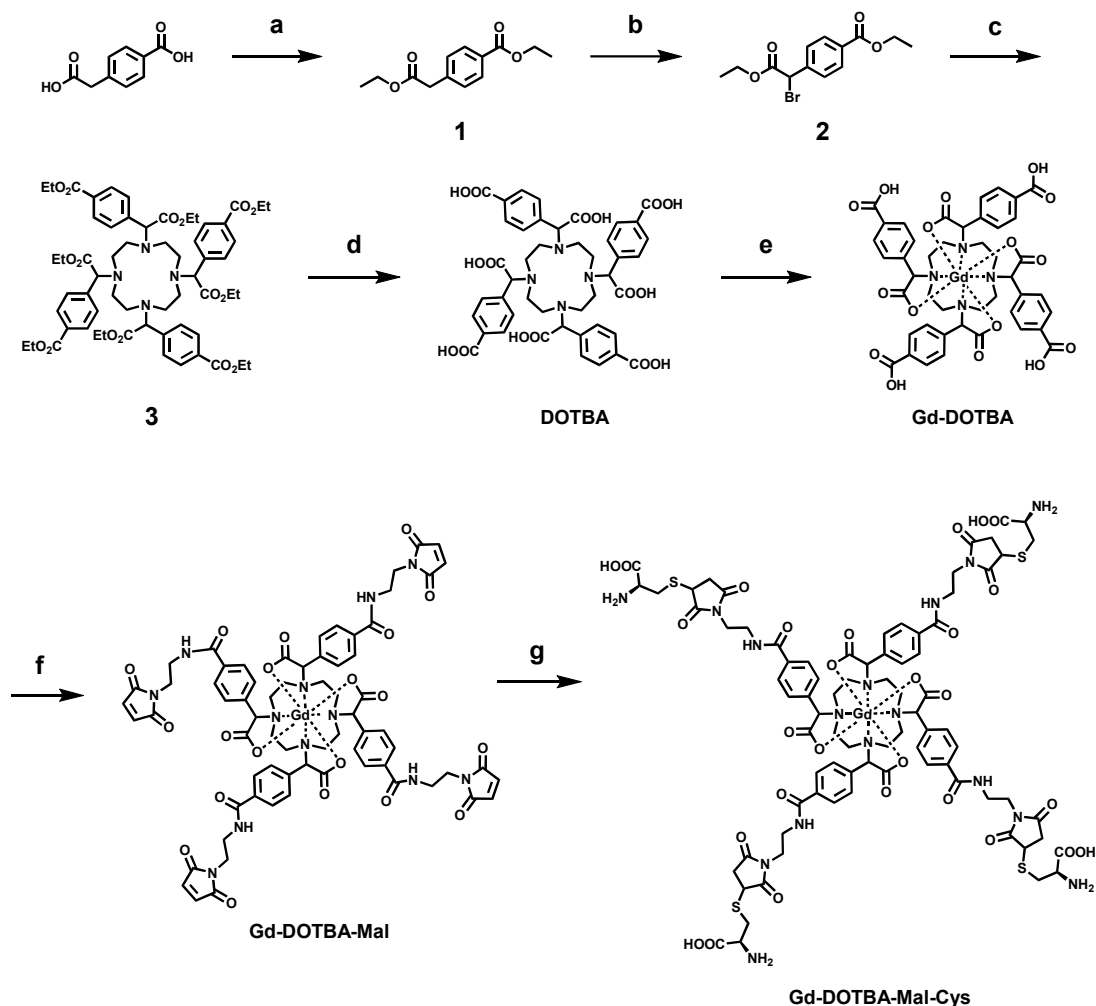
HPLC analysis was performed on a Waters Alliance e2695 system equipped with a C18 column (Waters, USA). Semi-preparative HPLC was carried out on a Waters system with a C18 column (19 \times 250 mm, Waters, USA). Mass spectrometry was performed on an Agilent 1290 Infinity II LC-MS system (Agilent, USA). Gd concentration was quantified using an Agilent 7850 ICP-MS (Agilent, USA). Relaxivity measurements were conducted on a 1.41 T benchtop NMR scanner (Huan Tong Nuclear Magnetic, China). *In vivo* magnetic resonance imaging was performed using a 3.0 T clinical MRI scanner (SIGNA, GE, USA). Microplate reader (EPOCH2NS, BioTek, USA) was used for absorbance measurements.

HPLC Methods

Analytical HPLC for all compounds was conducted at a flow rate of 1.0 mL/min using water with 0.1% TFA (Solvent A) and acetonitrile (Solvent B). The gradient profile was: 0–10 min, 10–100% B; 10–15 min, 100% B; returning to 10% B at 15 min. Preparative HPLC for **Gd-DOTBA-Mal** was performed at a flow rate of 7.0 mL/min using water with 0.1% TFA (Solvent A) and acetonitrile (Solvent B) with the following gradient: 0–10 min, 10–30% B; 10–30 min, 30–40% B; 30–33 min, 40–10% B. For the purification of **Gd-DOTBA-Mal-Cys**, preparative HPLC was carried out at 7.0 mL/min using 10 mM

ammonium acetate in water (Solvent A) and acetonitrile (Solvent B). The gradient was programmed as follows: 0–25 min, 10–80% B; 25–30 min, 80–10% B.

Synthesis



Scheme 1. Synthesis of Gd-DOTBA-Mal-Cys. (a) EtOH, conc. H_2SO_4 , reflux; (b) NBS, AIBN, CCl_4 , reflux; (c) cyclen, Cs_2CO_3 , ACN, reflux; (d) NaOH, H_2O , MeOH, reflux; (e) $\text{GdCl}_3 \cdot 6\text{H}_2\text{O}$, H_2O , reflux; (f) 1-(2-Aminoethyl)-1H-pyrrole-2,5-dione, DMTMM, H_2O , r.t.; (g) L-cysteine, PBS, r.t.

Gd-DOTBA was synthesized according to the reported procedures.^[1-2] During the ligand hydrolysis workup, the pH was adjusted to approximately 5, resulting in precipitation of the ligand as a white solid, which was collected by filtration, washed with water, and dried under vacuum (isolated yield > 90% over multiple batches).

Gd-DOTBA (1.57 g, 1.35 mmol), 1-(2-Aminoethyl)-1H-pyrrole-2,5-dione (0.95 g, 6.75 mmol), and DMTMM (1.86 g, 6.75 mmol) were dissolved in water (10 mL). The mixture was stirred at room temperature for 4 h under a nitrogen atmosphere and protected from light. The reaction was monitored by analytical HPLC. Upon completion, the mixture was filtered, and the filtrate was purified by preparative HPLC. The desired fractions were collected and lyophilized to afford the Gd-DOTBA-Mal as a white, fluffy solid. HPLC: $t_R = 5.474$ min (purity > 98%). MS (ESI): m/z calculated for $C_{68}H_{64}GdN_{12}O_{20}$ $[M+2H]^+$: 1528.3; found: 1528.2.

Gd-DOTBA-Mal (1.0 g, 0.65 mmol) and L-cysteine (0.39 g, 3.25 mmol) were dissolved in 1× PBS (10 mL). The reaction mixture was stirred overnight at room temperature under a nitrogen atmosphere. After the reaction was completed (monitored by analytical HPLC), the crude product was directly purified by preparative HPLC. Fractions containing the desired product were collected and lyophilized to afford **Gd-DOTBA-Mal-Cys** as a white powder. HPLC: $t_R = 4.356$ min (purity > 98%). HRMS (ESI): m/z calculated for $C_{80}H_{90}GdN_{16}O_{28}S_4$ $[M+2H]^+$: 2012.45482; found: 2012.45388.

Determination of Relaxivity

A 1.41 T MR magnet (60 MHz, Huan Tong Nuclear Magnetic, China) was used for longitudinal relaxation time (T_1) measurements. The 90° and 180° pulse durations were set at 40 μ s and 80 μ s, respectively. An inversion-recovery sequence with 10 inversion times logarithmically spaced between $0.05 \times T_1$ and $5 \times T_1$ was employed; the repetition time was 10.0 s. Gd-DOTBA-Mal-Cys was dissolved in UP water to achieve Gd^{3+} concentrations of 0, 0.1, 0.2, 0.3, 0.4, and 0.5 mM. A 200 μ L aliquot of each solution was transferred to an NMR tube and measured at 37°C. The longitudinal relaxivity (r_1) was obtained from the slope of the linear fit of $1/T_1$ versus Gd^{3+} concentration.

Determination of Gd Metal Content of Gd-DOTBA-Mal-Cys

The Gd content of the purified complex was determined by inductively coupled plasma mass spectrometry (ICP-MS). A precisely weighed amount of **Gd-DOTBA-Mal-Cys** powder was dissolved in 2% HNO₃ and diluted to a target Gd concentration of 200–500 µg/L based on the theoretical metal loading. The solution was filtered through a 0.22 µm membrane prior to analysis. Calibration standards were prepared by serial dilution of a 1000 mg/L Gd stock solution with 2% HNO₃. Each sample was measured in triplicate, and the average value was taken. The actual Gd content of the complex was calculated from the ratio of the measured concentration to the theoretical value.

Kinetic Stability Assessment

The kinetic stability of **Gd-DOTBA-Mal-Cys** was assessed via acid-assisted dissociation and transmetallation assays. The complex was dissolved in 1.0 M HCl (acidic condition, room temperature) or in PBS (10 mM, pH 7.4) containing 10 mM ZnCl₂ (transmetallation, 50 °C) at a final Gd³⁺ concentration of 1.0 mM. For each sample, 200 µL was transferred to an NMR tube and the T_1 was measured immediately at 37°C and 1.41 T as the initial value $T_1(t_0)$. The acid system was incubated at room temperature and the Zn²⁺ system at 50°C for 7 days. At predetermined time points, T_1 was remeasured. The normalized ratio $T_1(t)/T_1(t_0)$ as calculated and plotted against incubation time to evaluate kinetic stability.

Cell Cytotoxicity

The cytotoxicity of **Gd-DOTBA-Mal-Cys** against LX-2, 293T, and HeLa cells was evaluated via a standard CCK-8 assay. Cells were seeded in 96-well plates at a density of 5×10^3 cells/well and cultured for 24h. The medium was then replaced with fresh DMEM or 1640 medium containing various concentrations of **Gd-DOTBA-Mal-Cys** (0, 0.2, 0.4, 0.6, 0.8, 1.0 mM). After 24h of incubation, CCK-8 solution (10% v/v) was added and the plates were incubated for another 4h. The absorbance at 450 nm of each well was measured on a microplate reader.

Acute and Subacute Toxicity Assessment

To assess acute toxicity, The Balb/c mice received a single intravenous injection of Gd-DOTBA-Mal-Cys (0.1 mmol/kg), Gd-DOTA (0.1 mmol/kg), or PBS (n = 3 per group). After 24 h, organs (liver, kidney) were collected. For subacute toxicity, injections were given weekly for four weeks, with organ collection 24 h after the final dose. All tissues were fixed in 4% paraformaldehyde, embedded in paraffin, sectioned at 5 μ m thickness, and subjected to H&E staining for histological analysis.

Animal Model

All animal experiments were conducted under the Institutional Ethical Guidelines on Animal Care. All procedures were approved by the Institute of Animal Care and Use Committee at Wenzhou Institute, UCAS (WIUCAS25070203 and WIUCAS25091804). Female BALB/c mice (6–8 weeks, 17–20 g, Zhejiang Animal Center) were kept under specific pathogen free (SPF) conditions for one week prior to the experiments. Mice were anesthetized by intraperitoneal injection of 2% sodium pentobarbital before surgery. For the unilateral ureteral obstruction (UUO) model, the right side of the lower abdomen was sterilized and incised. The right ureter was freed with forceps, ligated at two points with non-absorbable sutures, and transected between the ligatures. The incision was closed. MRI scans were performed 2 and 9 days after ligation. In the sham-operated group, the right ureter was exposed but not ligated or transected; For the subcutaneous 4T1 model, 2.5×10^6 4T1 cells in 100 μ L PBS/Matrigel (1:1) were injected into the right flank. The needle was withdrawn, and gentle pressure was applied for 1 min to prevent leakage.

***In vivo* MRI Studies**

MRI was performed on a 3.0 T clinical scanner (SIGNA, GE) equipped with a dedicated mouse coil. Mice were anesthetized with 2% sodium pentobarbital. For

normal mice, **Gd-DOTBA-Mal-Cys** was injected via the tail vein at 0.1 mmol/kg. For UUU model mice (2 and 9 days post-surgery) and subcutaneous 4T1 tumor-bearing mice, a half dose of 0.05 mmol/kg was administered. T_1 -weighted images were acquired pre-injection and at serial time points using a fast spin-echo sequence with the following parameters: Freq. FOV = 6.0 cm, slice thickness = 1.5 mm, spacing = 0.2 mm, TR = 160.0 ms, TE = 4.9 ms, slices = 10. The signal-to-noise ratio (SNR) was measured by finely analyzing regions of interest (ROIs) of the longitudinal images, and the contrast enhancement was defined as the increase of SNR after the injection. The signal-to-noise ratio (SNR) was determined by selecting regions of interest (ROIs) on coronal or transverse slices. The enhancement was taken as the SNR increase following contrast administration, and the nSNR was subsequently derived to enable quantitative comparison of dynamic signal changes.

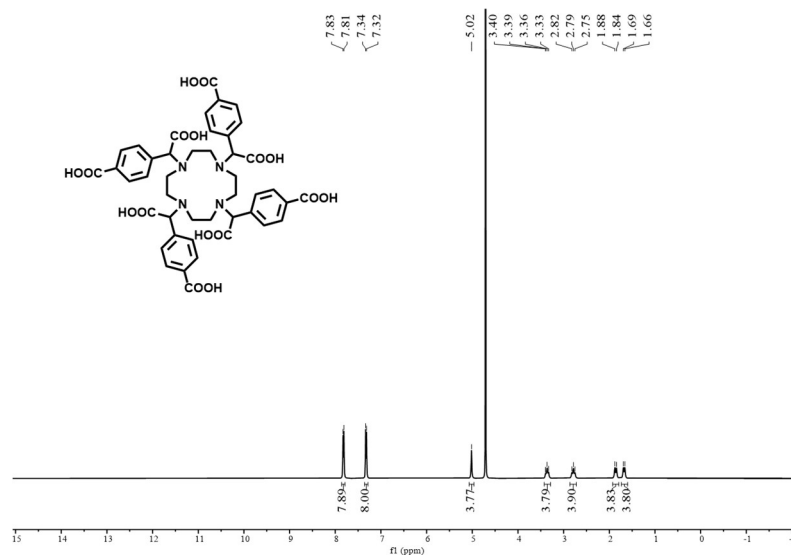
Biodistribution

Healthy female BALB/c mice were randomly assigned to three time-point groups (5 min, 15 min, and 24 h; n = 3 per group). Each mouse received a single intravenous injection of Gd-DOTBA-Mal-Cys at a dose of 0.1 mmol Gd/kg body weight. At the designated time points, animals were euthanized, and blood and major organs (heart, liver, spleen, lung, kidney, brain, small intestine, and hindlimb muscle) were harvested. Approximately 100 mg of each tissue sample was digested in concentrated HNO_3 until complete clarification was achieved. The digests were diluted with ultrapure water to a final HNO_3 concentration of 2% (v/v), filtered through a 0.22 μm membrane, and analyzed by ICP-MS. Gd concentrations were quantified using a standard calibration curve and expressed as μg Gd per g tissue.

Table S1 Relaxivity of **Gd-DOTBA-Mal-Cys**^a

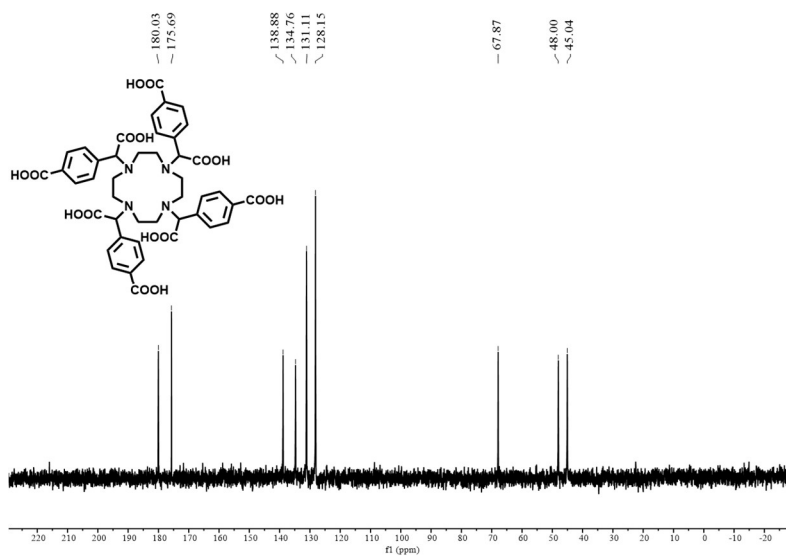
Complex	r_1 (in H ₂ O)	r_2 (in H ₂ O)	r_1 (in 4.5% HSA)	r_2 (in 4.5% HSA)
Gd-DOTBA-Mal-Cys	16.6 ± 0.2	19.3 ± 0.3	17.7 ± 0.1	21.2 ± 0.5

^aConditions: 37°C, 1.41 T; units, mM⁻¹ s⁻¹; HSA, human serum albumin (4.5%, w/v).



¹H NMR (400 MHz, Deuterium Oxide) δ 7.82 (d, J = 7.9 Hz, 8H), 7.33 (d, J = 7.8 Hz, 8H), 5.02 (s, 4H), 3.43 – 3.29 (m, 4H), 2.79 (t, J = 13.6 Hz, 4H), 1.86 (d, J = 14.3 Hz, 4H), 1.68 (d, J = 13.0 Hz, 4H).

Fig. S1 ¹H NMR spectrum of DOTBA in D₂O.



^{13}C NMR (100 MHz, Deuterium Oxide) δ 180.03, 175.69, 138.88, 134.76, 131.11, 128.15, 67.87, 48.00, 45.04.

Fig. S2 ^{13}C NMR spectrum of DOTBA in D_2O .

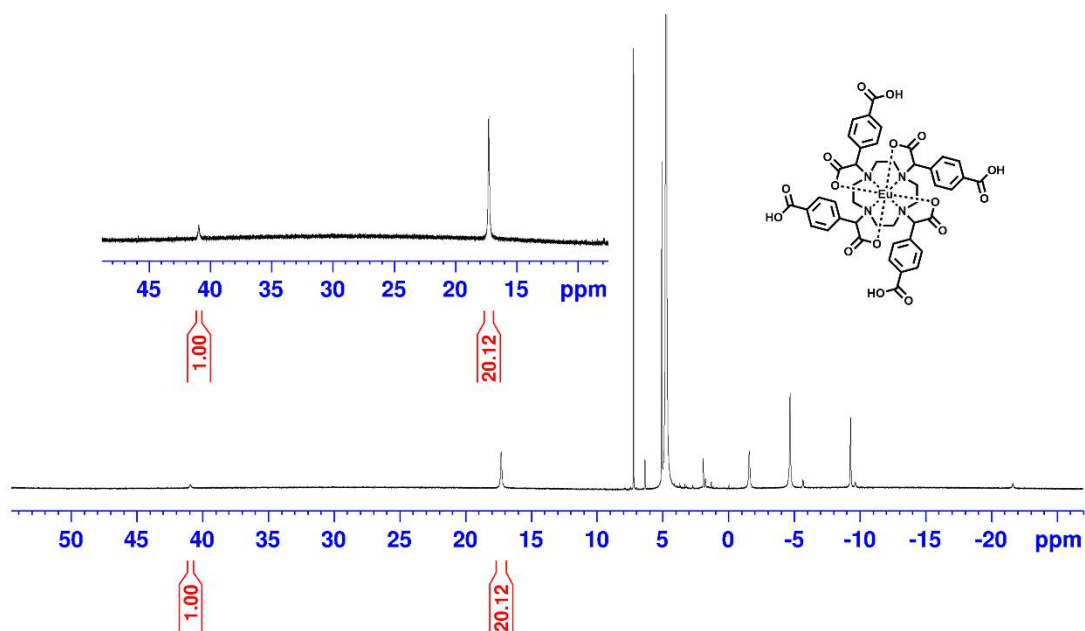


Fig. S3 ^1H NMR spectrum of Eu-DOTBA in D_2O .

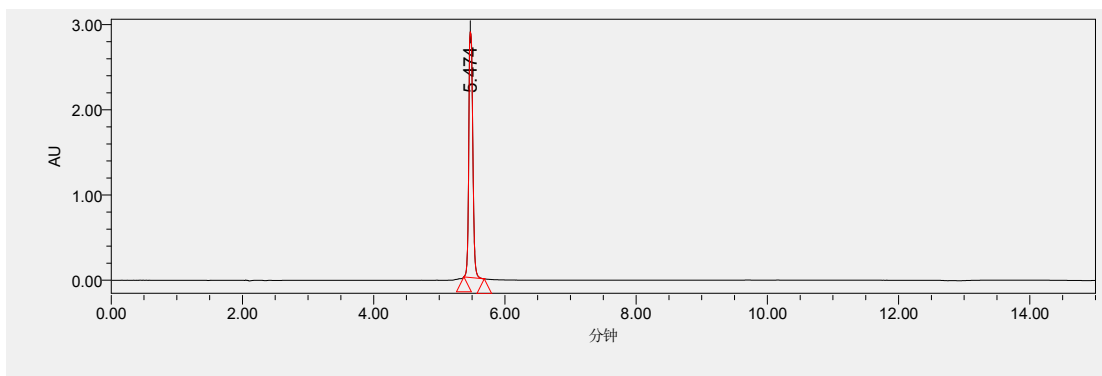


Fig. S4 Analytical HPLC spectrum of **Gd-DOTBA-Mal**.

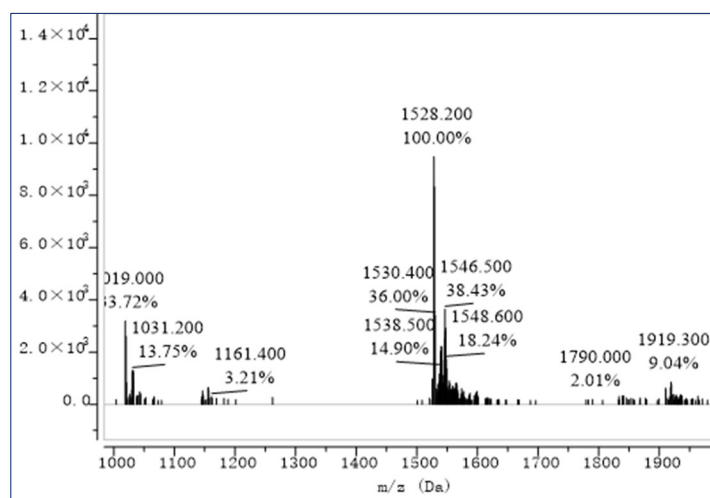


Fig. S5 ESI-MS of **Gd-DOTBA-Mal**.

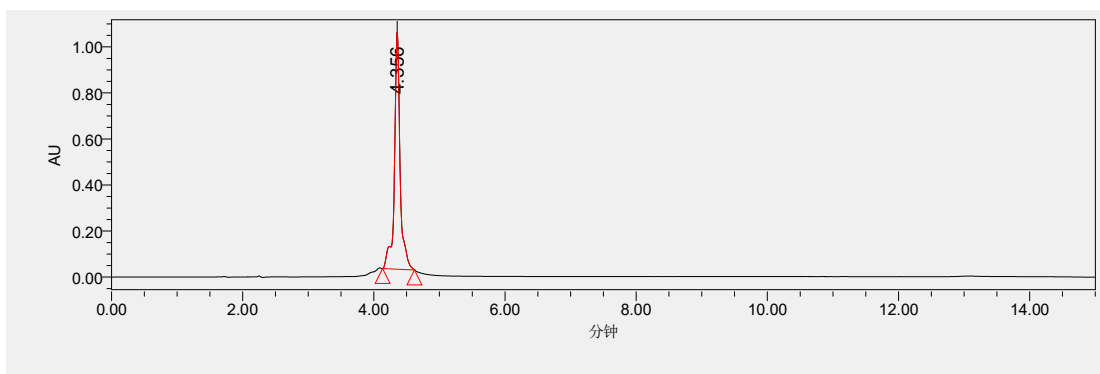


Fig. S6 Analytical HPLC spectrum of **Gd-DOTBA-Mal-Cys**.

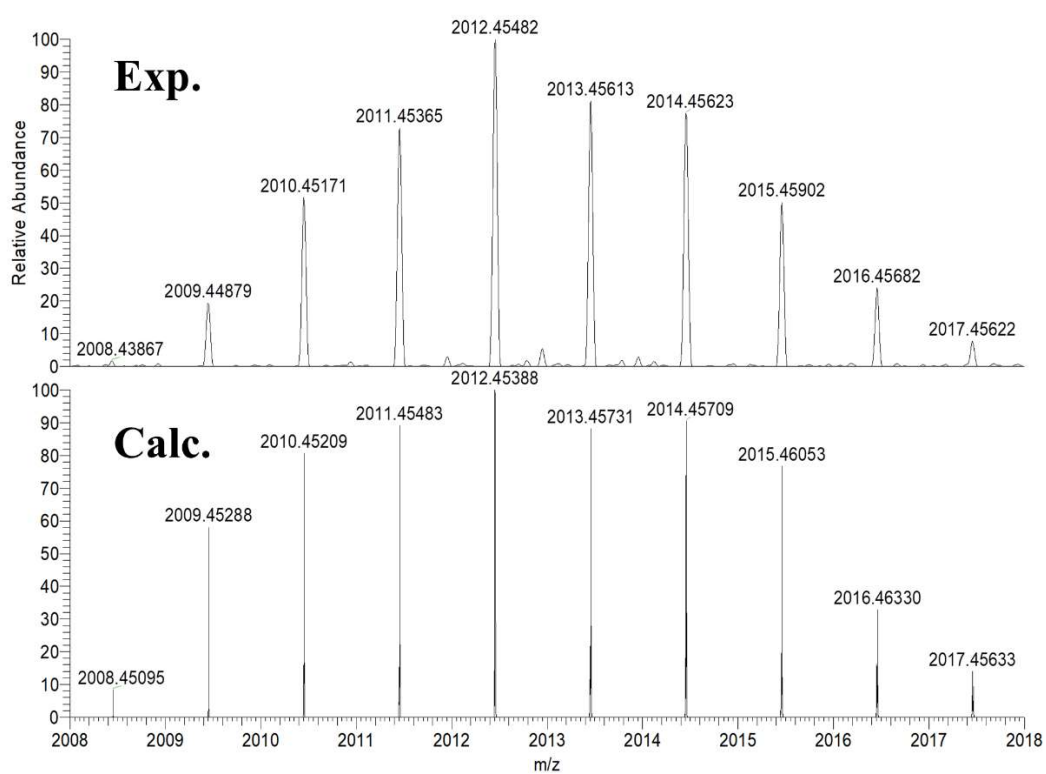


Fig. S7 High resolution ESI-MS of **Gd-DOTBA-Mal-Cys**.

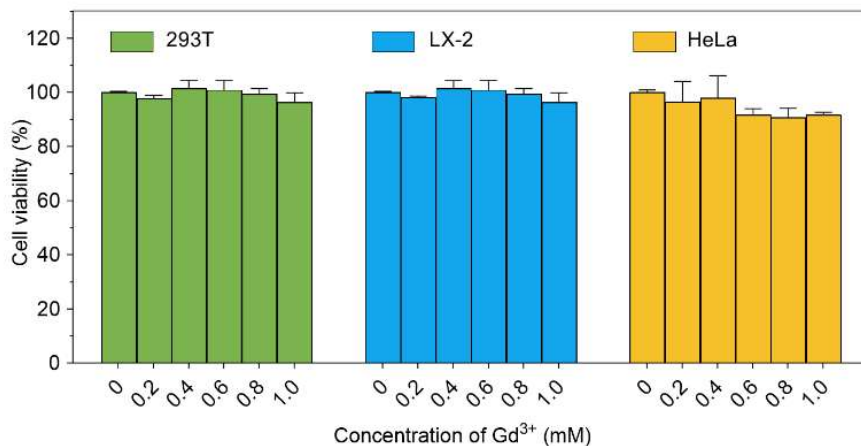


Fig. S8 Cell viability of LX-2, 293T, and HeLa cells after 24h incubation with varying concentrations of **Gd-DOTBA-Mal-Cys**.

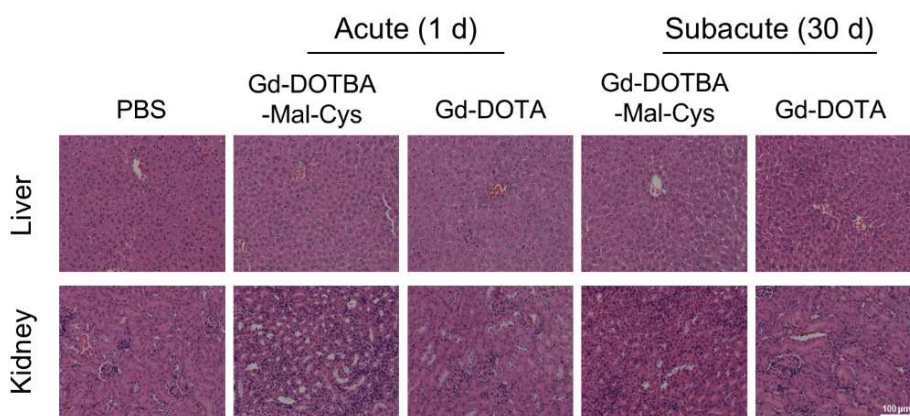


Fig. S9 Representative H&E-stained sections of liver and kidney from Balb/c mice treated with PBS, Gd-DOTA, or **Gd-DOTBA-Mal-Cys** (0.1 mmol/kg) in acute (1 day) and subacute (30 days) toxicity studies. Scale bar = 100 μm.

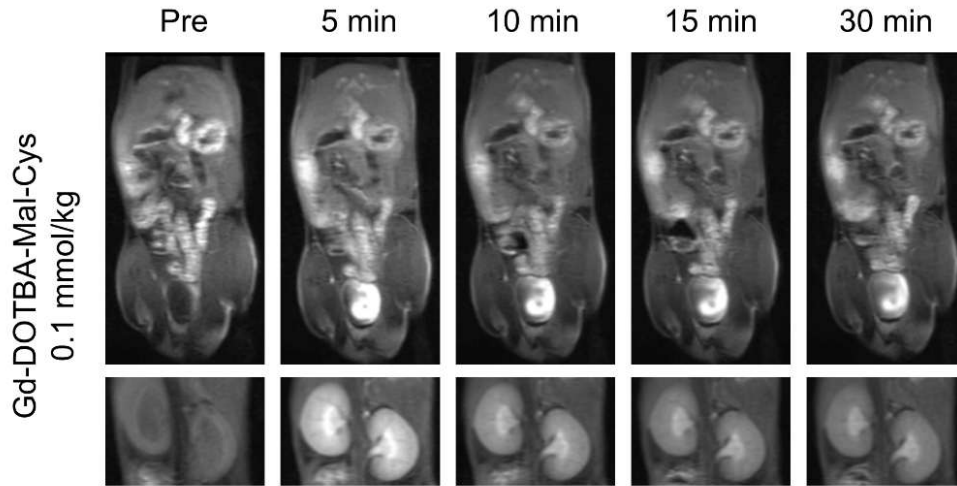


Fig. S10 T_1 -weighted MR images of normal mice at different time points after intravenous injection of **Gd-DOTBA-Mal-Cys** at 3.0 T magnetic field.

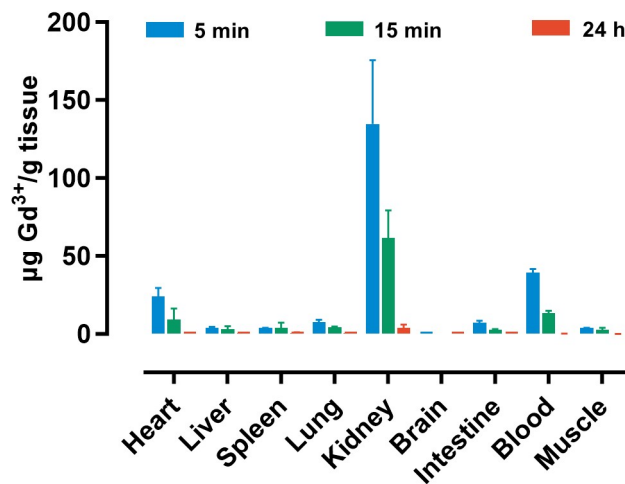


Fig. S11 Biodistribution of the **Gd-DOTBA-Mal-Cys**.

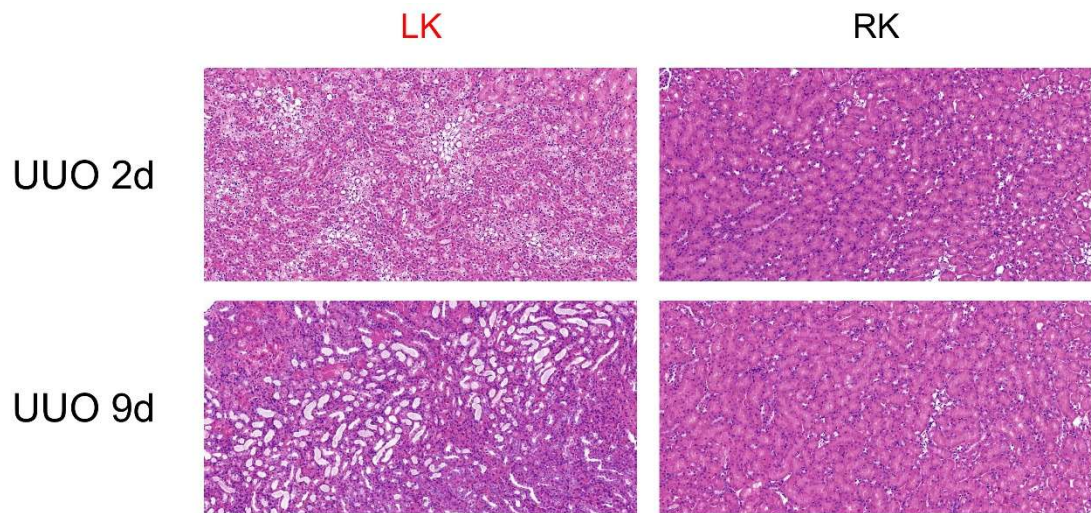


Fig. S12 HE-staining of the kidney after UUO 2days and UUO 9 days (scale = 200 μ m)

References

- [1] K. B. Maier, L. N. Rust, F. Carniato, M. Botta, M. Woods, *Chem. Commun.*, 2024, **60**, 2898-2901.
- [2] K. B. Maier, L. N. Rust, C. I. Kupara, M. Woods, *Chem. Eur. J.*, 2023, **29**, e202301887.